Environmental Research 240 (2024) 117470

Contents lists available at ScienceDirect

Environmental Research

journal homepage: www.elsevier.com/locate/envres

Morphological and metabolic changes in microglia exposed to cadmium: Cues on neurotoxic mechanisms

Federica Bovio [a], Elisa Perciballi [a], Pasquale Melchioretto [b], Daniela Ferrari [a], Matilde Forcella [a,*], Paola Fusi [a,c,**], Chiara Urani [b,c]

[a] Department of Biotechnology and Biosciences, University of Milano-Bicocca, Piazza della Scienza 2, 20126, Milan, Italy
[b] Department of Earth and Environmental Sciences, University of Milano- Bicocca, Piazza della Scienza 1, 20126, Milan, Italy
[c] Integrated Models for Prevention and Protection in Environmental and Occupational Health, Interuniversity Research Center, (MISTRAL), Italy

ARTICLE INFO

Handling Editor: Jose L Domingo

Keywords:
Cadmium
Microglia
Energetic metabolism
Oxidative stress
Mitochondria

ABSTRACT

Microglial cells play a key role in protecting the central nervous system from pathogens and toxic compounds and are involved in the pathogenesis of different neurodegenerative diseases. Cadmium is a widespread toxic heavy metal, released into the environment at a rate of 30,000 tons/year by anthropogenic activities; it is easily uptaken by the human body through diet and cigarette smoke, as well as by occupational exposure. Once inside the body, cadmium enters the cells and substitutes to zinc and other divalent cations altering many biological functions. Its extremely long half-life makes it a serious health threat. Recent data suggest a role for heavy metals in many neurodegenerative diseases; however, the role of cadmium is still to be elucidated. In this work we report the investigation of cadmium toxicity towards murine BV2 microglial cells, a widely used model for the study of neurodegeneration. Results show that increasing cadmium concentrations increase oxidative stress, a proposed mechanism of neurodegeneration, but also that BV2 cells can keep oxidative stress under control by increasing glutathione reduction. Moreover, cadmium induces alterations of cell morphology and metabolism leading to mitochondrial impairment, without switching the cells to Warburg effect. Finally cadmium induces the release of proinflammatory cytokines, but does not markedly switch BV2 cells to M1 phenotype.

1. Introduction

Microglia, the brain resident macrophages, normally play the role of immune monitoring and are key mediators of nervous system pathology development and progression (Wright-Jin and Gutmann, 2019). As central nervous system (CNS) sentinels, microglia detect and respond to a diverse array of stimuli in the brain, including environmental toxins. They are highly metabolically active cells, changing their metabolism upon stimulation and during neurodegeneration (Rangaraju et al., 2018). In their M2 phenotype, microglia are immunosuppressive, display a branched morphology and use oxidative metabolism for energy production; whereas the switching to the M1 phenotype leads to change in their morphology to an amoeboid structure, to the increase phagocytic activity, impaired oxidative phosphorylation and increased glycolysis (Borst et al., 2019). Activated microglia surrounds lesions of various neurodegenerative diseases, such as Alzheimer's disease (AD), Parkinson's disease (PD), amyotrophic lateral sclerosis (ALS), and multiple sclerosis. Microglia have been shown to be activated by different heavy metals, including cadmium (Martínez-Hernández et al., 2023).

Although cadmium has been used in the past at very high concentrations (100 μM) for neurophysiological studies as calcium-channel blocker (Kim-Lee et al., 1992), human exposure, accumulation and its possible role in neurotoxicity and neurodegeneration have been neglected since more recent years.

Cadmium is a non-essential heavy metal with a well-known toxicity in humans (Genchi et al., 2020), currently listed as the seventh most hazardous chemical for human health, considering both toxicity and exposure frequency (ATSDR, 2022). Besides occupational exposure, cadmium can be assumed by the general population through cigarette smoke, the diet and polluted air (Garner and Levallois, 2016; Hartwig and Jahnke, 2017; Sarwar et al., 2010) and it accumulates inside the human body, particularly in the liver and kidney, with a half-life of 25–30 years, due to the lack of excretion pathways (Sarkar et al., 2013).

* Corresponding author. Department of Biotechnology and Biosciences, University of Milano-Bicocca, Piazza della Scienza 2, 20126, Milan, Italy.
** Corresponding author. Department of Biotechnology and Biosciences, University of Milano-Bicocca, Piazza della Scienza 2, 20126, Milan, Italy.
E-mail addresses: matilde.forcella@unimib.it (M. Forcella), paola.fusi@unimib.it (P. Fusi).

https://doi.org/10.1016/j.envres.2023.117470
Received 6 September 2023; Received in revised form 9 October 2023; Accepted 20 October 2023
Available online 21 October 2023

Upon chronic exposure, cadmium can reach very high concentrations inside the human body, as in the aortic wall of heavy smokers (20 cigarettes/day), where it has been found at a maximum concentration of 20 μM (Abu-Hayyeh et al., 2001). Thanks to its structural similarity with zinc, cadmium easily enters the cells with a mechanism known as "Trojan horse" (Martelli et al., 2006), exploiting zinc transporters and calcium channels (Genchi et al., 2020; Thévenod et al., 2019). Once inside the cells cadmium readily displaces zinc, as well as copper and iron, in different proteins, inducing oxidative stress, DNA damage, endoplasmic reticulum (ER) stress, mitochondrial dysfunction and autophagy (Ma et al., 2022; Tang et al., 2021).

Neurotoxic effects have recently been described for cadmium (Ruczaj and Brzóska, 2023; Wang and Matsushita, 2021), since it accumulates in different brain areas (Wang and Du, 2013), particularly in the *locus ceruleus* neurons of patients with different clinicopathological conditions and causes of death (Pamphlett et al., 2018). Environmental exposure to this metal has been suggested to damage the nervous system and to be involved in the etiopathogenesis of neurodegenerative diseases, such as Alzheimer's disease, Parkinson's disease and amyotrophic lateral sclerosis (Oggiano et al., 2021; Ruczaj and Brzóska, 2023). Moreover, cadmium has been shown to induce apoptosis in motor neurons of cultured explants from human fetal spinal cords (Sarchielli et al., 2012) and in the olfactory bulbs of experimental animals exposed to this metal through diet or inhalation (Sunderman, 2001). Although acute cadmium exposure is blocked by the blood-brain barrier (BBB), following chronic exposure cadmium has been shown to increase the permeability of the BBB (Branca et al., 2020). Interestingly, the olfactory bulb represents a direct route for cadmium uptake, bypassing the intact BBB (Wang and Du, 2013). More recently, several studies have shown that cadmium can lead to cognitive impairment (Deng et al., 2023; Lillehoj et al., 2019; Sasaki and Carpenter, 2022) and to the activation of the JAK2/STAT3 signaling pathway. This is a signal transduction pathway that can be regulated by various cytokines, and participates in the proliferation, survival, and differentiation of nerve cells in the CNS. It also plays important roles in mediating inflammation, immune response, synaptic plasticity, neurodegeneration, and memory formation (Liu et al., 2023). On the other hand, the inhibition of the Wnt/β-catenin signaling, a pathway playing crucial roles in many biological processes including neurodevelopment, and microglial activation, has been found to induce alterations of zebrafish neurobehavior, thereby potentially presenting one of the key targets of cadmium neurotoxicity (Xu et al., 2022).

Yang and coworkers (Yang et al., 2007) demonstrated that cadmium induces microglial activation through the production of ROS and the activation of transcription factors sensitive to redox states, like NF-κB and AP-1, which leads to the expression of genes related to oxidative stress. Another study conducted both in vivo and *in vitro* showed that, in the BV2 murine microglial cell line, cadmium increased the levels of p–NF–κB, which plays a central role in inflammation through its ability to induce transcription of proinflammatory genes (Khan et al., 2019). Moreover, very recently, cadmium has been shown to induce mitochondrial dysfunction in neuronal cells, through SIRT1 mediated-oxidative stress (Wen et al., 2023).

In a previous work on human SH-SY5Y neuronal cell line we have demonstrated that early cadmium exposure caused alterations in the oxidative balance with an increase in glycolysis and in glutamine dependency (Bovio et al., 2021). In addition, our previous work confirmed the molecular mimicry of cadmium and its role in metals' unbalance as the possible initial event in neurotoxicity (Forcella et al., 2022).

In this work we addressed our attention to the microglial sensitive component of the CNS and we report an investigation of cadmium morpho-functional effects towards BV2 murine microglial cells, an *in vitro* model in neurodegeneration studies, and already used in pharmaceutical industry (Henn et al., 2009). We focused on cell metabolism and defense mechanisms against oxidative stress as possible co-players in the processes of cadmium neurotoxicity.

2. Materials and methods

2.1. Mammalian cell culture

BV2 murine microglia cells, kindly donated by Professor Maria D'Erme from University of Rome "La Sapienza", were grown in DMEM medium supplemented with heat-inactivated 10% FBS, 4 mM L-glutamine, 100 U/mL penicillin, 100 μg/mL streptomycin and maintained at 37 °C in a humidified 5% CO_2 incubator. For the experimental work BV2 cells were not used above passage 10.

All the reagents for cell culture were supplied by EuroClone (Pero, Milan, Italy).

2.2. Cell viability assay

For the evaluation of cadmium toxicity on cell viability, the *in vitro* toxicology assay kit MTT-based was used according to manufacturer's protocols (Merck KGaA, Darmstadt, Germany).

The absorbance was measured at 570 nm using VICTOR Multilabel Plate Reader (PerkinElmer, Waltham, MA, USA) and cell viability is expressed as a percentage against viability of untreated cells. Each experiment was performed in three replicate wells for each $CdCl_2$ concentration and results are presented as the mean of at least three independent experiments.

2.3. Cell staining for morphological evaluation

To evaluate cadmium effect on microglia cell morphology, BV2 were seeded at a density of 7×10^4 cells/35 mm dish and 24 h after the seeding exposed to 1 μM, 5 μM, 10 μM or 20 μM $CdCl_2$. After 24 h all dishes were fixed and stained with Giemsa solution as previously reported (Bovio et al., 2021). Cells were then observed by light microscopy at 10 × and 40 × magnification, using Zeiss Axioplan microscope equipped with digital camera.

2.4. Metallothioneins extraction and expression

BV2 cells were seeded at 1×10^6 cells/100 mm dish with 2 dishes for each experimental condition and 24 h after the seeding were exposed to 0–20 μM $CdCl_2$. After 24 h of treatment the cells were processed for metallothioneins extraction according to Forcella et al. (2020)

Subsequently, 20 μg of total proteins were separated on gradient 4–12% gel (Invitrogen Thermo Fisher Scientific) and transferred to nitrocellulose. Western blotting was performed according to Urani et al. (2010) using a mouse anti-metallothionein antibody (Zymed, Thermo Fisher Scientific), diluted 1:1000, that binds MT-I and MT-II isoforms and a mouse anti-vinculin (diluted 1:5000, Merck KGaA, Darmstadt, Germany) as a loading control.

Densitometric analysis by Scion Image software (Scion Corp. Fredrick, Walkersville, MD, USA) provided the quantification of protein expression (MTs) in cadmium treated samples compared to controls.

All chemicals were purchased from Merck KGaA, Darmstadt, Germany.

2.5. Western blot analysis

To examine cadmium effect on glycolytic and mitochondrial targets, BV2 cells were seeded at 5×10^5 cells/60 mm dish and 24 h later treated with 1–20 μM $CdCl_2$ (untreated cells represent the control). Following the 24 h treatment the cells were rinsed with ice-cold PBS and lysed in RIPA buffer containing 1 μM leupeptin, 2 μg/mL aprotinin, 1 μg/mL pepstatin and 1 mM PMSF. After lysis on ice, homogenates were obtained by passing 5 times through a blunt 20-gauge needle fitted to a syringe and centrifuged at 14,000×*g* for 15 min. Supernatants were analyzed for protein content by the BCA protein assay (Smith et al., 1985).

SDS-PAGE and Western blot were performed by standard procedures with 40 μg of proteins separated on 12 or 15 % acrylamide/bis-acrylamide SDS-PAGE and transferred onto a nitrocellulose membrane (Millipore, Billerica, MA, USA) (Laemmli, 1970). Subsequently the nitrocellulose membrane was blocked in a 5% (w/v) dried milk-PBS solution for 1 h and incubated overnight at 4 °C with the appropriate primary antibodies. The following primary antibodies were used: anti-HMOX1 (dilution 1:1000, Enzo Biochem Inc, Framingdale, NY, USA), anti-PKM2 (dilution 1:1000, Cell Signaling Technology, Danvers, MA, USA), anti-PFKFB3 (dilution 1:1000, Cell Signaling Technology, Danvers, MA, USA), anti-GAPDH (dilution 1:1000, Cell Signaling Technology, Danvers, MA, USA), anti-OPA1 (dilution 1:1000, Cell Signaling Technology, Danvers, MA, USA) and anti-MFF (dilution 1:1000, Cell Signaling Technology, Danvers, MA, USA), with anti-vinculin (dilution 1:5000, Merck KGaA, Darmstadt, Germany) and anti-β-tubulin (dilution 1:5000, Merck KGaA, Darmstadt, Germany) as loading control. After three washing (10 min each) in PBS-0.3% (v/v) Tween 20, the membrane was incubated for 1 h with anti-mouse IgG HRP-conjugated secondary antibodies diluted 1:8000 or anti-rabbit IgG HRP-conjugated secondary antibodies diluted 1:5000 (Cell Signaling Technology, Danvers, MA, USA). After three washing (10 min each) in PBS-0.3% (v/v) Tween 20, proteins were visualized using ECL detection system (EuroClone, Pero, Milan, Italy), according to the manufacturer's instructions. Protein levels were quantified by densitometry of immunoblots using ImageJ software (National Institute of Health, USA). All chemicals were purchased from Merck KGaA, Darmstadt, Germany.

2.6. Lipid peroxidation assay

The extent of lipid peroxidation was determined by the levels of malondialdehyde (MDA) measured using the thiobarbituric acid reactive substances assay (Buege and Aust, 1978). BV2 cells were seeded at 1×10^6 cells/100 mm dish and, on the following day, were treated with 1 μM, 5 μM, 10 μM or 20 μM $CdCl_2$, while untreated cells represent the control. Twenty-four hours after the treatment, the samples were prepared according to Bovio et al. (2021). Lipid peroxidation level was expressed as nmol of MDA/mg protein using a molar extinction coefficient of 1.56×10^5 M^{-1} cm^{-1}. Results were reported as a percentage compared to untreated control and results are presented as the mean of at least three independent experiments.

All chemicals were supplied by Merck KGaA, Darmstadt, Germany.

2.7. Glutathione detection

The measurement of total glutathione (GSH tot), oxidized glutathione (GSSG) and reduced glutathione (GSH) content was carried out on microglia cells treated with $CdCl_2$ for 24 h. In detail, BV2 cells were seeded in 6-well plates at a density of 2×10^5 cells/well and, the day after seeding, exposed to $CdCl_2$ (1–20 μM) for 24 h, with cells not treated with $CdCl_2$ representing the control. At the end of the treatment, the cells were harvested by trypsinization and washed with PBS, the resulting pellet weighed and then lysed in 200 μL of 1% SSA (Sulfosalicylic acid).

For total glutathione measurement, 10 μL of each cell lysate, in triplicate, were transferred into a new 96-well plate and 90 μL of MilliQ water were added; then, 100 μL of reaction mixture (100 μM DTNB (5,5′-dithiobis(2-nitrobenzoic acid)), 200 μM NADPH, 0.46 U/mL glutathione reductase, 100 mM Na_2HPO_4, 100 mM NaH_2PO_4, pH 7.5) were added to each well and absorbance at 405 nm was measured immediately as well as after 20 min using a VICTOR Multilabel Plate Reader (PerkinElmer, Waltham, MA, USA). Additionally, a calibration curve was prepared (0–10 μM GSH) and treated like the samples.

For GSSG evaluation 100 μL of cells lysate were transferred into a new tube and treated with 2 μL of 2-vinylpyridine solution (27 μL 2-vinylpyridine in 98 μL ethanol) for 1 h at RT in order to block the SH-groups. Subsequently 10 μL of each cell lysate, in triplicate, were added to 90 μL of MilliQ water on a new 96-well plate followed by 100 μL of reaction mixture and absorbance at 405 nm was measured immediately as well as after 20 min using a microplate reader. Additionally, a calibration curve was prepared (0–10 μM GSSG) and treated like the samples.

The values of absorbance were compared to standard curves, converted into molarity for both total glutathione and GSSG and normalized on pellet weight, expressed in mg, while GSH has been calculated by subtracting GSSG to total glutathione (GSH = GSH tot − GSSG). GSSG and GSH were expressed as a percentage of total glutathione for each condition. Each experiment was performed in triplicate per metal concentration for each biological replicate and at least three independent biological replicates were carried out.All chemicals were supplied by Merck KGaA, Darmstadt, Germany.

2.8. Enzyme activity assays

In order to evaluate the effect of cadmium on glutathione S-transferase (GST), glutathione reductase (GR), glucose-6-phosphate dehydrogenase (G6PDH), isocitrate dehydrogenase (ICDH), malic enzyme (ME), pyruvate kinase (PK), lactate dehydrogenase (LDH) and malate dehydrogenase (MDH) activities, BV2 cells were seeded at 1×10^6 cells/100 mm dish and, 24 h later, exposed to 1–20 μM $CdCl_2$ for 24 h, with untreated cells representing the control. At the end of the treatment, cells were rinsed with ice-cold PBS (10 mM K_2HPO_4, 150 mM NaCl, pH 7.2) and lysed in 50 mM Tris/HCl, pH 7.4, 150 mM NaCl, 5 mM EDTA, 10% glycerol, 1% NP40 buffer, containing 1 μM leupeptin, 2 μg/mL aprotinin, 1 μg/mL pepstatin and 1 mM PMSF (phenylmethylsulfonyl fluoride). After lysis on ice, homogenates were obtained by passing the cells 5 times through a blunt 20-gauge needle fitted to a syringe and then centrifuging at 15,000×*g* at 4 °C for 30 min. The resulting supernatant was used to measure GST activity according to Habig et al. (1974), GR activity according to Wang et al. (2001) and G6PDH, ICDH, ME, PK, LDH, MDH activities according to Bergmeyer (Bergmeyer et al., 1974).

Enzyme activities were expressed in international units and referred to protein concentration, quantified by Bradford assay, using BSA for the calibration curve (Bradford, 1976). All assays were performed at 30 °C in technical duplicate for each biological replicate and at least three independent biological replicates have been carried out.

All chemicals were purchased by Merck KGaA, Darmstadt, Germany.

2.9. Seahorse analysis

BV2 cells were seeded in Agilent Seahorse 96-well XF cell culture microplates at a density of 5×10^3 cells/well in 180 μL of growth medium, allowed to adhere for 24 h in a 37 °C humidified incubator with 5% CO_2 and treated with $CdCl_2$ 1 μM, 5 μM, 10 μM or 20 μM for 24 h. Untreated cells represent the control. In addition, before running the assay, the Seahorse XF Sensor Cartridge was hydrated and calibrated with 200 μL of Seahorse XF Calibrant Solution in a non-CO_2 37 °C incubator.

Mitochondrial functionality, glycolysis and ATP production were investigated using the Agilent Seahorse XF Cell Mito Stress Test Kit, Agilent Seahorse XF Glycolysis Stress Test Kit and the Agilent Seahorse XF ATP Rate Assay Kit, respectively.

Each experiment was performed in technical quadruplicate per metal concentration for each biological replicate and at least three independent biological replicates have been carried out. Data were normalized on total protein content, quantified by Bradford assay (Bradford, 1976).

All the kits and reagents were purchased by Agilent Technologies, Santa Clara, CA, USA.

2.10. Mitochondrial immunofluorescence staining

BV2 cells were seeded in 24-well plates at a density of 1.5×10^4 cells/well on poly-L-lysine coated (0.001 % water solution) glass

coverslips. After 24 h, cells were treated with different $CdCl_2$ concentrations (1–20 μM) for additional 24 h. The day after treatment cells were washed with HBSS, stained with 100 nM PhenoVue TM 551 Mitochondrial stain (PerkinElmer, Waltham, MA, USA) for 30 min, washed again with HBSS and then fixed with 4 % paraformaldehyde (PFA) for 15 min. Subsequently cells were washed three times with PBS, permeabilized with 0.1 % Triton X-100-PBS solution for 10 min, stained with anti-β-tubulin (dilution 1:1000, Merck KGaA, Darmstadt, Germany) and nuclei were counterstained for 10 min with 1 μg/mL Hoechst-PBS solution (Merck KGaA, Darmstadt, Germany). After three washes in PBS coverslips were mounted using FluorSave TM Reagent (Calbiochem, San Diego, CA, USA) on microscope slides and images were acquired with a Nikon A1R confocal microscope of the PMib center at the University of Milano-Bicocca (Nikon, Tokyo, Japan). Confocal

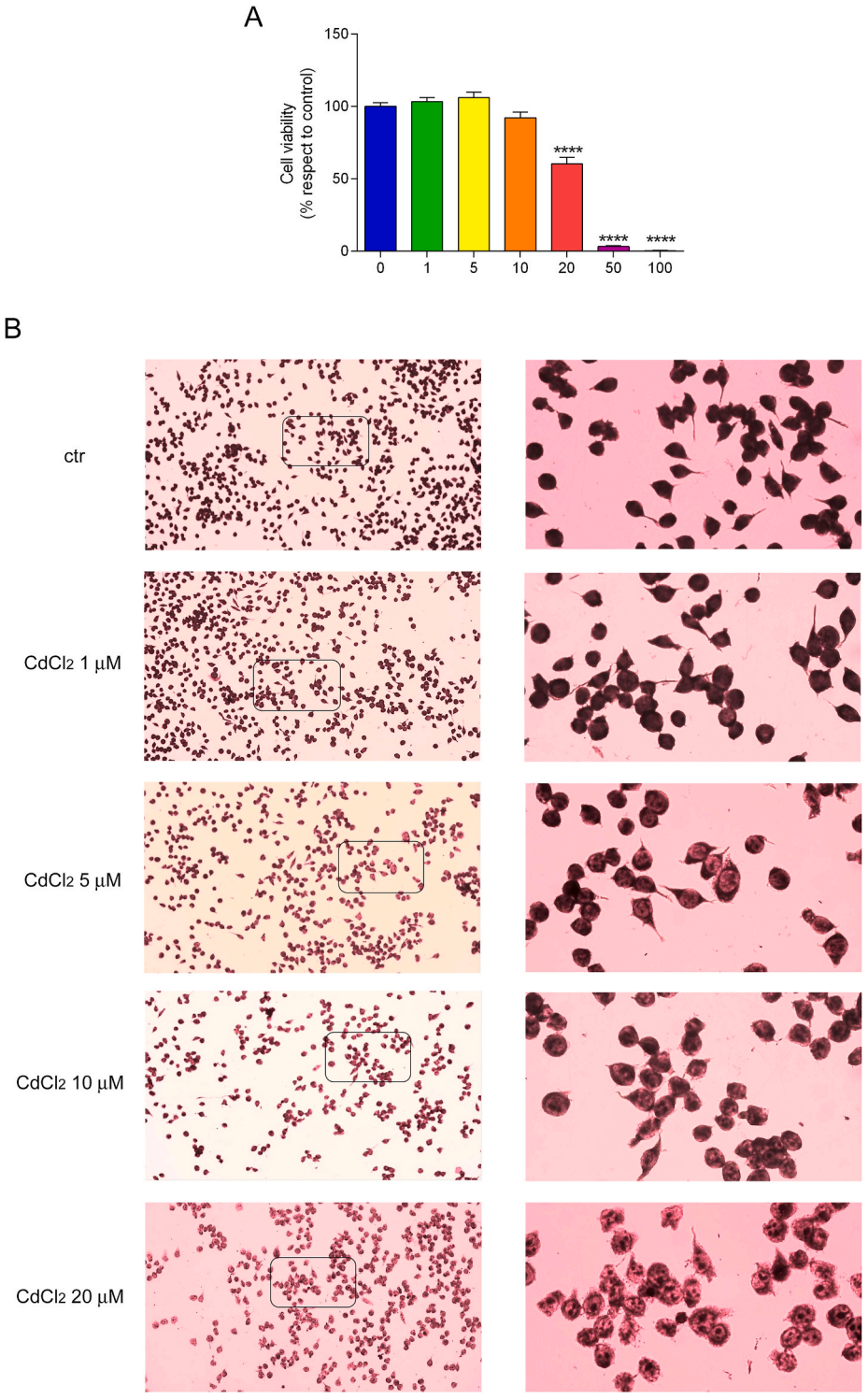

Fig. 1. BV2 viability and morphology following a 24-h cadmium treatment. (A) Cell survival was determined by MTT assay in the presence of different $CdCl_2$ concentrations (0–100 μM). Data are shown as mean ± standard error (SEM) of at least three biological replicates. ****$p < 0.0001$ (B) Cell morphology of BV2 control cells (ctr) and cadmium treated cells were observed by light microscopy at 10 × and 40 × magnification after fixing and Giemsa staining. The right panel represents the squared region of the left panel observed at 40 × magnification.

images have been acquired with the same settings across experimental groups.

2.11. Determination of gene expression level by quantitative reverse transcription (qRT-PCR)

BV2 cells were seeded at a density of 5×10^5 cells/60 mm dish and after 24 h were treated with 1, 5, 10 or 20 μM $CdCl_2$ for 24 h. The total RNA was isolated using Quick-RNATM MiniPrep (Zymo Research, Irvine, CA, USA), and subsequently reverse-transcribed using Super-Script II Reverse Transcriptase (Invitrogen, Carlsbad, CA, USA), oligo dT and random primers, according to the manufacturer's protocol.

For quantitative real-time PCR (qPCR), 50 ng cDNA was PCR amplified with Luna® Universal qPCR Master Mix (New England Bio-Labs, Hitchin, Hertfordshire, UK) and specific primers, with an initial denaturation step at 95 °C for 10 min, followed by 40 cycles of 95 °C for 15 s and 59 °C annealing for 1 min, and the expression level of pro-inflammatory (IL-6, IL-1β and TNFα) and anti-inflammatory (IL-4 and IL-10) cytokines was evaluated (ABI 7500 Real-time PCR System, Applied Biosystem, Waltham, MA, USA). Each sample was normalized using the β-actin gene as an internal reference control. The relative expression level was calculated with the Livak method (2[-ΔΔC(T)]) and was expressed as a relative fold change between cadmium treated and untreated cells (Livak and Schmittgen, 2001).

The primers used for qPCR are the following: IL-6 Fw 5′-AGCCA-GAGTCCTTCAGAGAGA-3′ and Rv 5′-TGGTCTTGGTCCTTAGCCAC-3′; IL-1β Fw 5′-ACTCATTGTGGCTGTGGAGA-3′ and Rv 5′-TTGTTCATCTCGGAGCCTGT-3'; TNFα Fw 5′-TGAGCACA-GAAAGCATGACC-3′ and Rv 5′-AGGGTCTGGGCCATAGAACT-3'; IL-4 Fw 5′-AACGAGGTCACAGGAGAAGG-3′ and Rv 5′-TCTGCAGCTCCAT-GAGAACA-3'; IL-10 Fw 5′-ATAACTGCACCCACTTCCCA-3′ and Rv 5′-GGGCATCACTTCTACCAGGT-3'; β-actin Fw 5′-CCACCATGTACCCAGG-CATT-3′ and Rv 5′-CGGACTCATCGTACTCCTGC-3′.

2.12. Statistical analysis

All the experiments were carried out at least in biological triplicate, and the data were compared to their reference controls and analyzed using a one-way ANOVA followed by a Dunnet post hoc test. Results were considered statistically significant at $p < 0.05$.

3. Results

3.1. Treatment with increasing cadmium concentrations leads to morphological changes in BV2 cells

After 24 h cadmium treatment, BV2 cells showed a reduction in cell viability, as well as changes in cell morphology (Fig. 1). As shown in Fig. 1a, $CdCl_2$ administration (1–100 μM) decreased cell viability, although not in a classical dose-dependent way: viability was found comparable to control at lower doses (1–10 μM), while at 20 μM $CdCl_2$ a 40 % reduction was observed, reaching zero at 100 μM $CdCl_2$. Therefore, all the subsequent analyses were carried out at 1 μM, 5 μM, 10 μM and 20 μM, to provide better evidence of cadmium effects at low non-cytotoxic concentrations, simulating a chronic exposure.

At increasing $CdCl_2$ concentrations, cell morphology of BV2 glial cells showed significant changes under light microscopy (Fig. 1B). Despite no differences were observed between control cells (ctr) and the lowest cadmium concentration (1 μM), morphological changes were evident starting from 5 μM $CdCl_2$.

At higher cadmium concentrations, the cells exhibited an increased soma size, a more irregular and flattened morphology, evidenced by the visible area of the nucleus (40 × magnification), and an increase in the formation of filopodia-like small processes and blebs instead of branches.

3.2. Cadmium treatment leads to an increase in oxidative stress rescued by glutathione

Metallothioneins (MT) represent the first line of defense against divalent metal toxicity; in fact, their presence could be detected only in cadmium treated cells, with a dose-dependent increase in their expression till 6-fold at 20 μM $CdCl_2$ (Fig. 2A).

Regarding oxidative stress, HMOX1 expression, membrane lipid peroxidation, glutathione content, as well as antioxidant enzymes were evaluated in BV2 cells following a 24-h cadmium treatment. HMOX1 expression started to increase at 5 μM $CdCl_2$ and a significant 2-fold increase was reported in cells treated with 10 μM and 20 μM cadmium (Fig. 2A); on the contrary membrane lipid peroxidation strongly increased after treatment with 5 μM $CdCl_2$ and decreased at higher cadmium concentrations, with the level at 10 μM $CdCl_2$ still significantly higher than control cells, while the level at 20 μM $CdCl_2$ was 50 % lower than in untreated cells (Fig. 2B).

As reported in Fig. 2C, total intracellular glutathione concentration did not change following cadmium addition. On the contrary the content of oxidized GSSG and reduced scavenging GSH varied among samples: in fact, only at 5 μM $CdCl_2$ we observed a significantly higher GSSG content, matched by lower GSH compared to control cells: at any other dose GSSG and GSH content were similar to untreated cells (Fig. 2D). This suggests that the oxidative stress induced by cadmium at 5 μM concentration depletes GSH, which is then restored at the higher cadmium doses probably by the upregulation of glutathione S-transferase (GST) and glutathione reductase (GR) activity. In Fig. 2E and F GST and GR activity showed a significant increase at 10 μM and 20 μM $CdCl_2$, which can effectively counteract the oxidative stress induced by higher cadmium levels.

3.3. Cadmium alters mitochondrial oxygen consumption

Previous data on cadmium inhibition of the electron transport chain (Brand, 2016), as well as our results, led us to investigate mitochondrial functionality through Seahorse technology. While mitochondria treated with either 5 μM or 10 μM $CdCl_2$ did not differ from control cells in OCR and ECAR profiles; at 1 μM $CdCl_2$ a significant increase in both maximal respiration and spare respiratory capacity, as well as in mitochondrial ATP production OCR and ECAR profiles, was observed (Fig. 3A–C). On the other hand, at the highest cadmium dose, both OCR and ECAR profiles were lower than control (Fig. 3A–C). However, despite these differences, both control and treated cells showed no difference in mitochondrial coupling efficiency (data not shown). Moreover, Krebs cycle appears to be unaffected in all samples, since the malate dehydrogenase (MDH) activity was found to be similar to control at 1 μM, 10 μM and 20 μM $CdCl_2$ and significantly higher at 5 μM $CdCl_2$ (Fig. 3E). Finally, a 24-h cadmium treatment did not induce mitochondrial fission or fusion as documented by Western blot analysis of MFF and OPA1, respectively (Fig. 3D).

Mitochondrial distribution was further investigated through confocal microscopy, staining functional mitochondria with PhenoVue, as well as nuclei and tubulin. As shown in Fig. 4, tubulin staining confirmed that cell morphology is altered by cadmium, with cells becoming more elongated at increasing cadmium concentrations. Moreover, while control cells appear very homogeneous, cadmium treated cells showed increasing heterogeneity. When mitochondria were also stained with PhenoVue (Fig. 4), a different subcellular localization became evident, with mitochondria densely packed around the nuclei.

3.4. Cadmium impairs ATP production in BV2 cells, without leading to warburg effect

BV2 cells treated for 24 h with 5 μM, 10 μM and 20 μM $CdCl_2$ concentrations showed a decrease in total ATP production, significant from 10 μM $CdCl_2$, suggesting a major impairment of cell metabolism induced

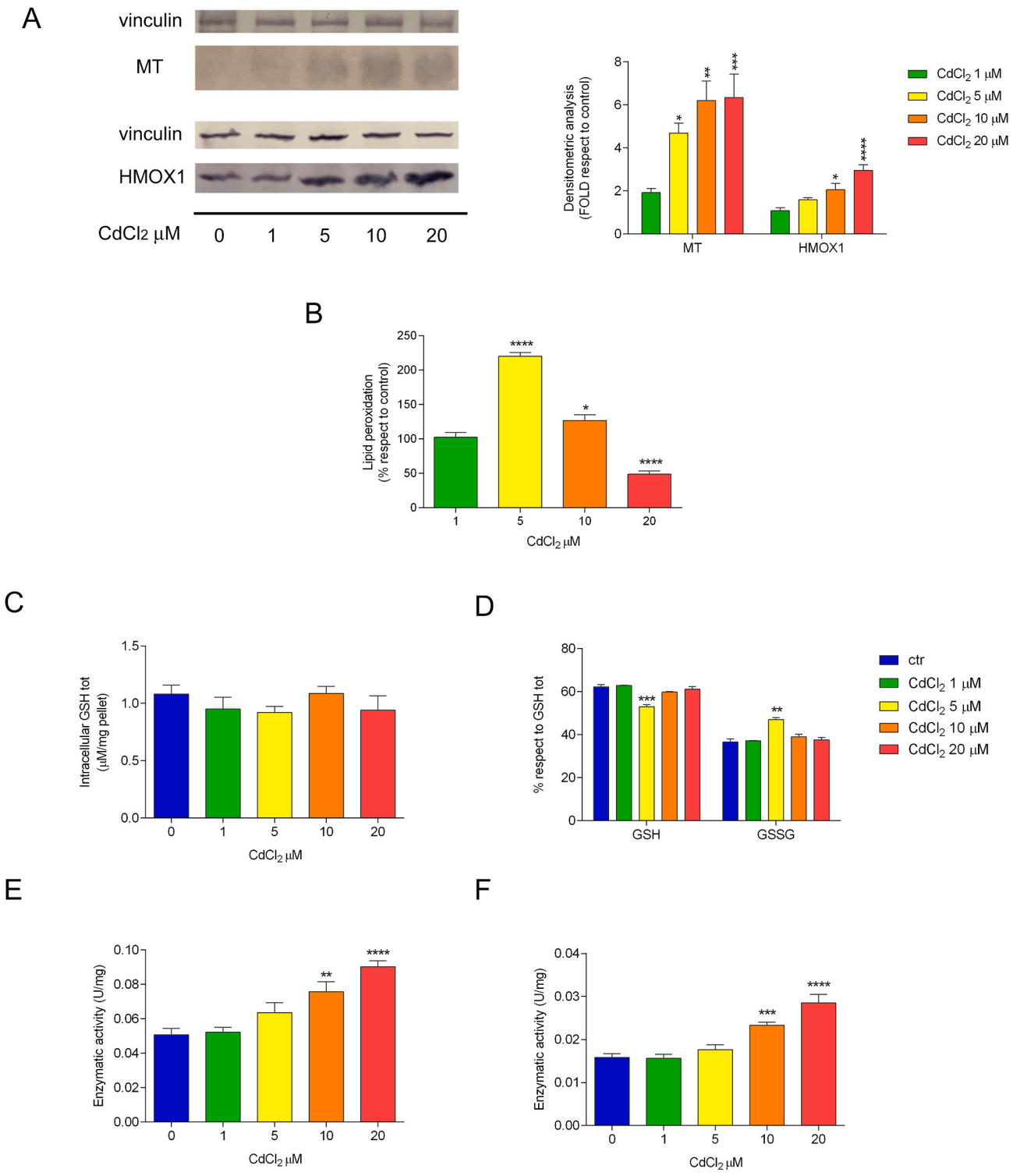

Fig. 2. Oxidative stress status following cadmium administration. (A) MT and HMOX1 protein expression in metal treated cells expressed as fold compared to control. (B) Lipid peroxidation level of cadmium treated cells expressed as a percentage of the control. (C) Total glutathione level expressed as µM/mg pellet. (D) GSSG and GSH contents expressed as percentages of total glutathione in cadmium treated and untreated cells. Enzyme activities of glutathione S-transferase (E) and glutathione reductase (F) in BV2 control and cadmium treated cells. Data are shown as mean ± standard error (SEM) of three biological replicates. *$p < 0.05$, **$p < 0.01$, ***$p < 0.001$, ****$p < 0.0001$ for all graphs.

by high cadmium concentrations (Fig. 5). When the different contributions of glycolysis and oxidative phosphorylation to ATP synthesis were calculated, mitochondrial ATP production was seen to decrease only at 20 µM $CdCl_2$, as previously determined in the OCR profile, while glycolytic ATP was found to significantly increase at 1 µM $CdCl_2$ and to decrease at higher cadmium concentrations, starting from 5 µM $CdCl_2$ (Fig. 5).

The ECAR profile, obtained by adding glucose to the medium followed by oligomycin and 2-DG did not show any significant difference in cells treated with different cadmium concentrations, except for a

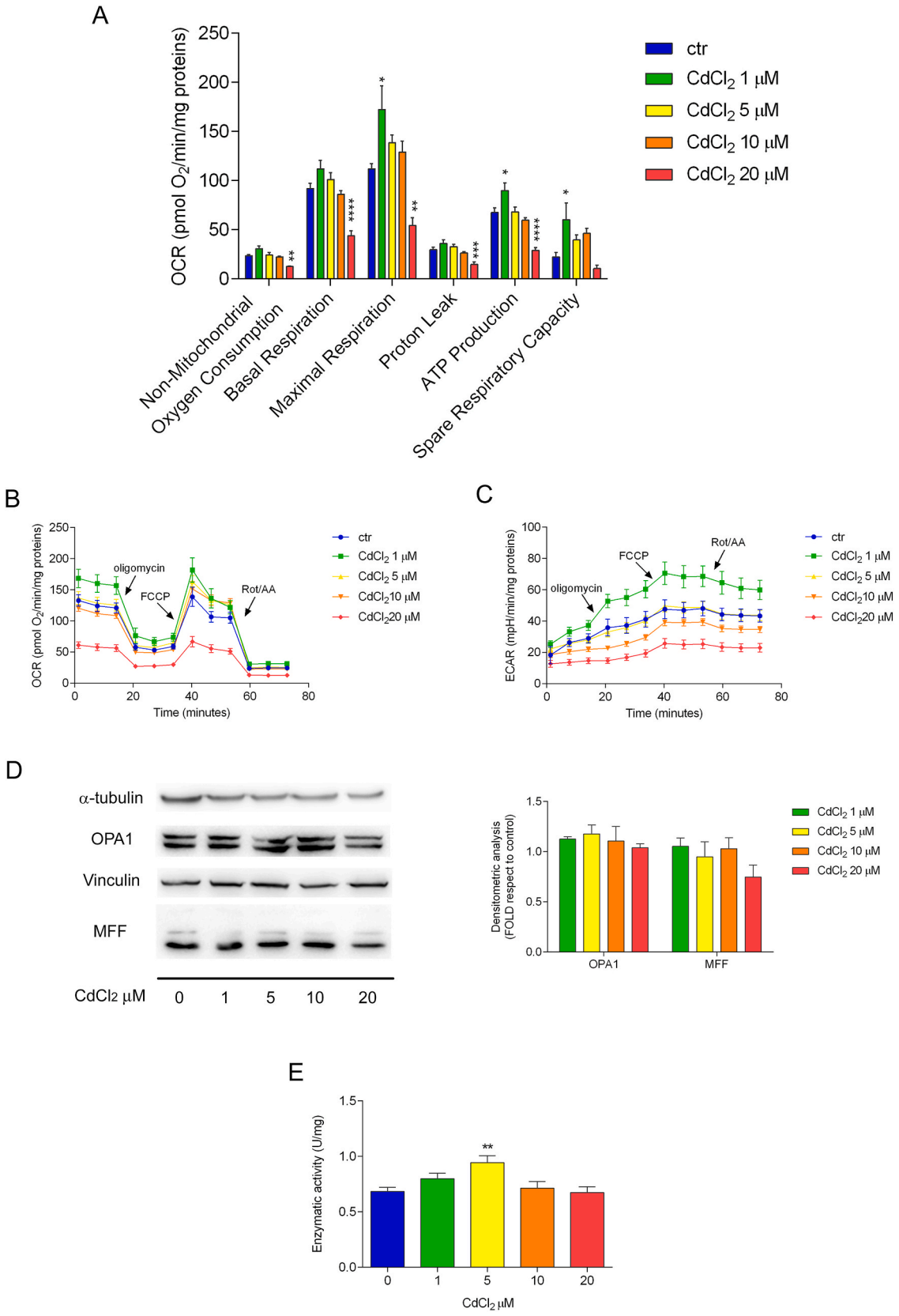

Fig. 3. Mitochondrial functionality of BV2 cells treated with cadmium. (A) Analysis of key mitochondrial parameters following the sequential addition of 1 µM oligomycin, 2 µM FCCP and 1 µM rotenone and antimycin A. OCR (B) and ECAR (C) profiles, expressed as pmol O_2/min/mg proteins and mpH/min/mg proteins respectively, in control and cadmium treated cells. (D) Representative Western blot analysis of OPA1 and MFF and their expression levels in metal treated cells expressed as fold compared to control. (E) Enzymatic activity of malate dehydrogenase in BV2 control and cadmium treated cells. Data are shown as mean ± standard error (SEM) of at least three biological replicates. *$p < 0.05$, **$p < 0.01$, ***$p < 0.001$, ****$p < 0.0001$ for all graphs.

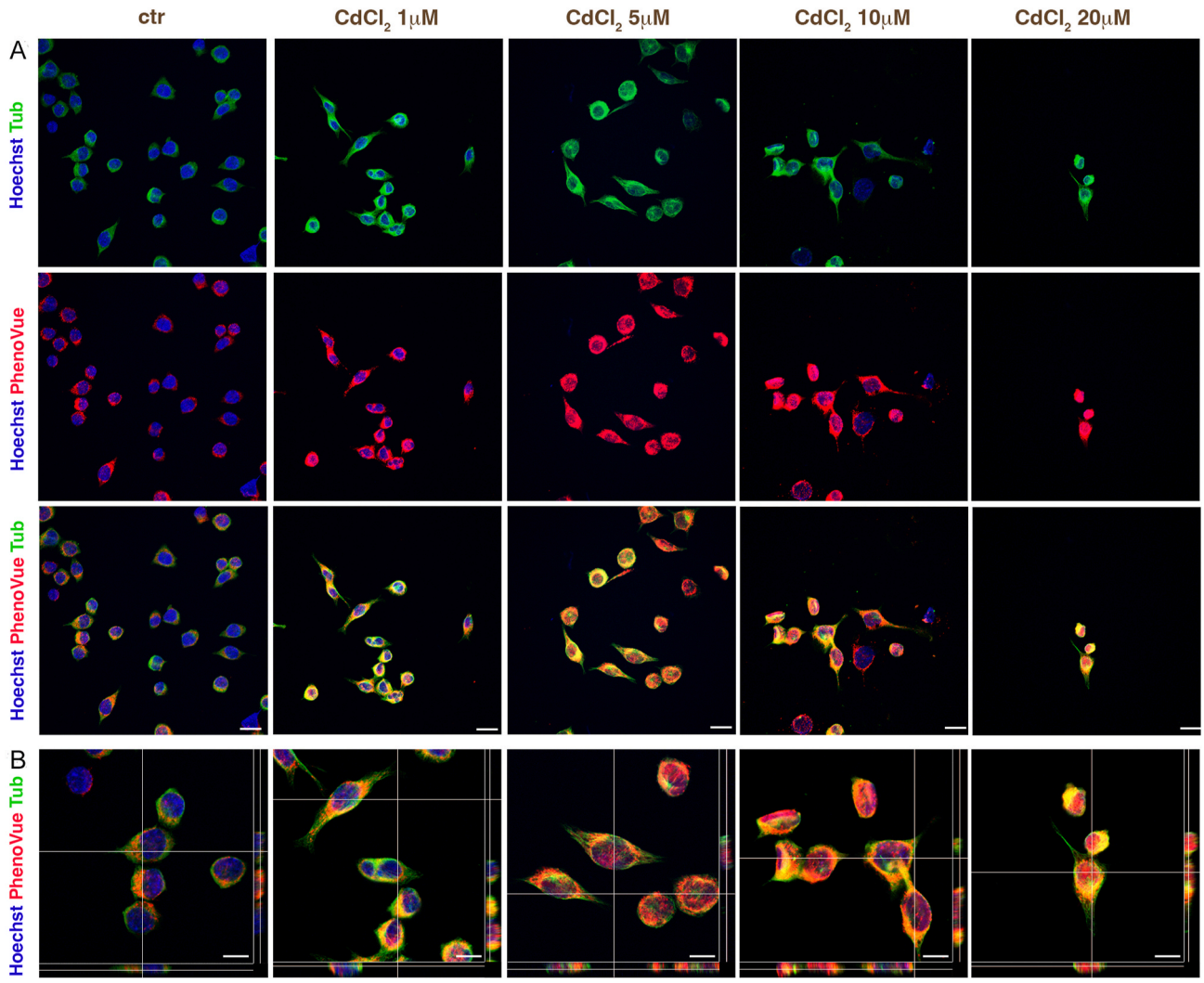

Fig. 4. Mitochondrial distribution in BV2 cadmium treated cells. Representative confocal images, showing the effect of increasing concentration of $CdCl_2$ on microglial cells morphology (panel A and B, tub, green) and mitochondria localization (panel A and B, PhenoVue, red). Nuclei were counterstained with Hoechst (blue). Scale bars: panel a, 20 μm; panel b, 10 μm.

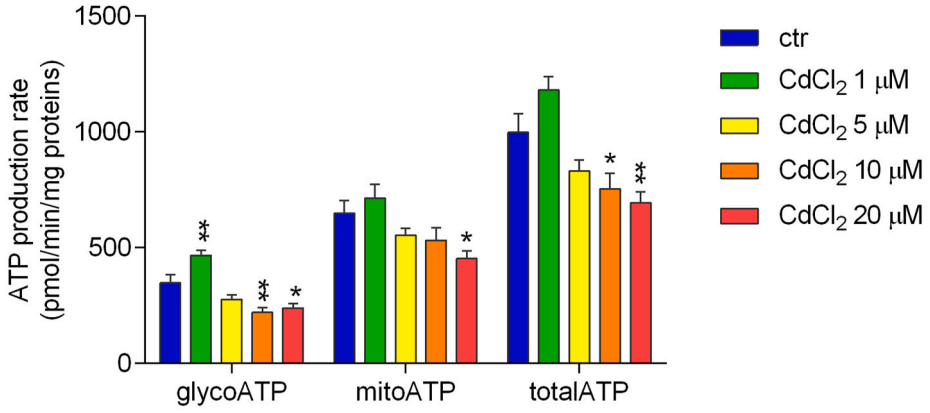

Fig. 5. ATP production in cadmium treated cells. Glycolytic, mitochondrial and total ATP production rate in microglial cells treated for 24 h with $CdCl_2$, measured with the Agilent Seahorse XF ATP Rate Assay Kit by adding 1.5 μM oligomycin followed by 1 μM rotenone and antimycin A. Bars indicate the mean ± SEM of three biological replicates. Statistically significant: *$p < 0.05$, **$p < 0.01$.

decrease in glycolytic capacity and reserve, observed at 20 μM $CdCl_2$ (Fig. 6A and B). However, a decreasing trend could be observed, starting from 5 μM $CdCl_2$, while treatment with 1 μM $CdCl_2$ induced an increase in both glycolytic capacity and glycolytic reserve, although not statistically significant. The activity of pyruvate kinase (PK) was found significantly higher in cadmium treated cells, with an activity twice

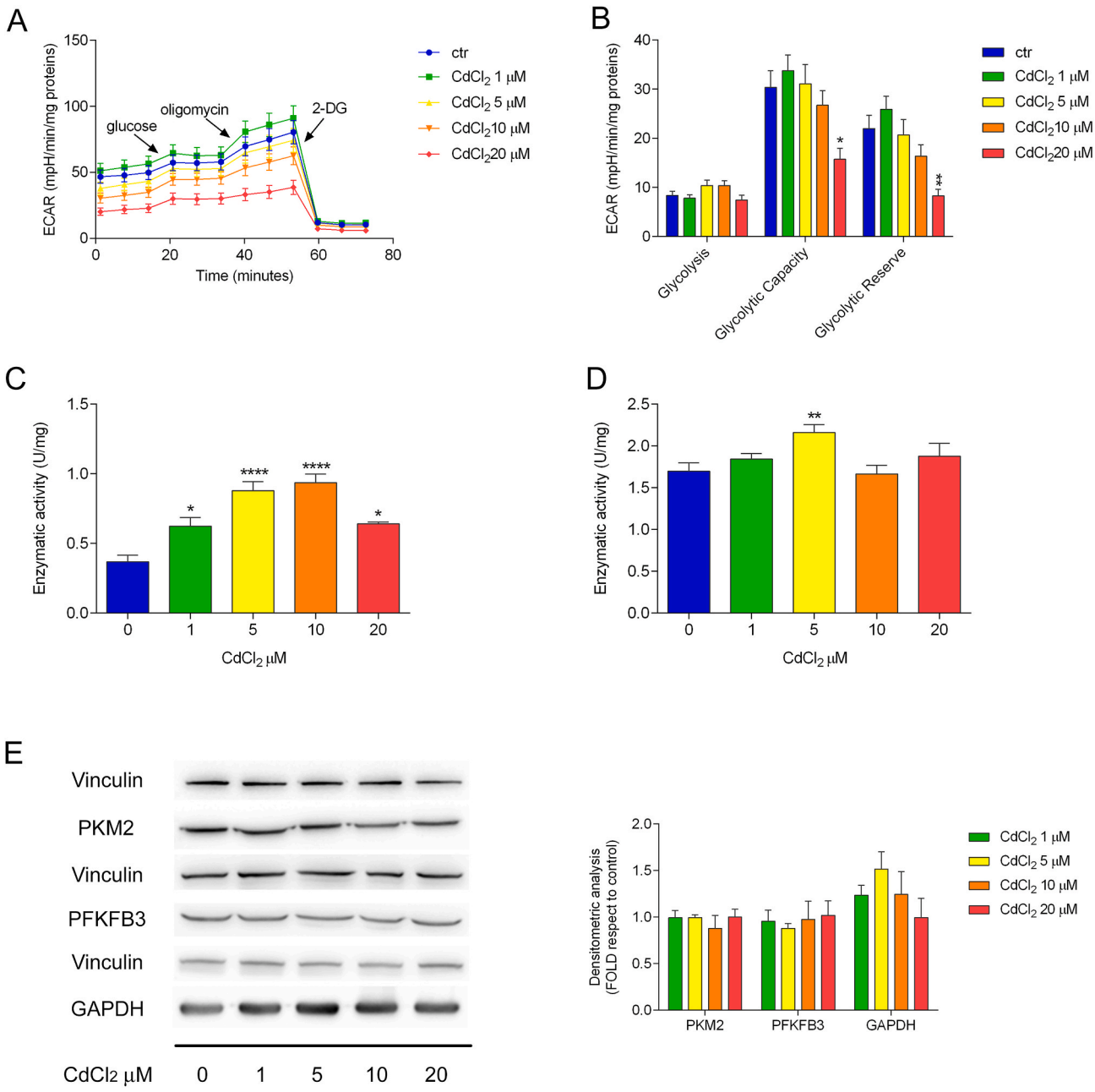

Fig. 6. Glycolytic functions analysis in BV2 cadmium treated cells. ECAR profile expressed as mpH/min/mg proteins (A) and analysis of different glycolytic parameters (B) of control and $CdCl_2$-treated cells. The arrows indicate the addition of 10 mM glucose, 1 µM oligomycin and 50 mM 2-DG. Enzyme activities of pyruvate kinase (C) and lactate dehydrogenase (D) in BV2 control and cadmium treated cells. (E) Representative Western blot analysis of PKM2, PFKFB3 and GAPDH and their expression levels in metal treated cells expressed as fold compared to control. Bars indicate the mean ± SEM of three biological replicates. *p < 0.05, **p < 0.01, ****p < 0.0001 for all graphs.

higher at 5 µM and 10 µM $CdCl_2$, while lactate dehydrogenase (LDH) was observed to be similar to control in all cadmium treated cells except at 5 µM $CdCl_2$, where it significantly increased as shown in Fig. 5C and D. However, no differences were detected in the expression of PFBK3 and PKM2 isoforms, which are normally upregulated in Warburg effect, and only a non-significant increase was observed in GAPDH protein expression at 5 µM $CdCl_2$ (Fig. 6E).

As reported in Fig. 7A, no significant differences were detected in the expression of glucose 6-phosphate dehydrogenase (G6PDH), suggesting no upregulation of the pentose phosphate shunt. While for the other two enzymes involved in NADPH production, we observed a non-statistically significant increase in isocitrate dehydrogenase (ICDH) activity at lower cadmium doses and a significant increase in malic enzyme activity at 1 µM $CdCl_2$, followed by a decreasing trend, statistically significant only at 20 µM $CdCl_2$ (Fig. 7B and C).

3.5. Cadmium effect on pro-inflammatory interleukins is heterogeneous

Although data obtained showed impairment of mitochondrial functionality at the highest cadmium doses, BV2 cells morphology and glycolysis alterations do not suggest a switch to the inflammatory M1 phenotype. To assess cadmium ability to induce this switch, the expression of pro-inflammatory (IL-6, IL-1β and TNFα) and anti-inflammatory (IL-4 and IL-10) cytokines was analyzed through real-time PCR. Results, reported in Fig. 8A, showed how treatment with the highest cadmium concentration induced a 4-fold increase of IL-6

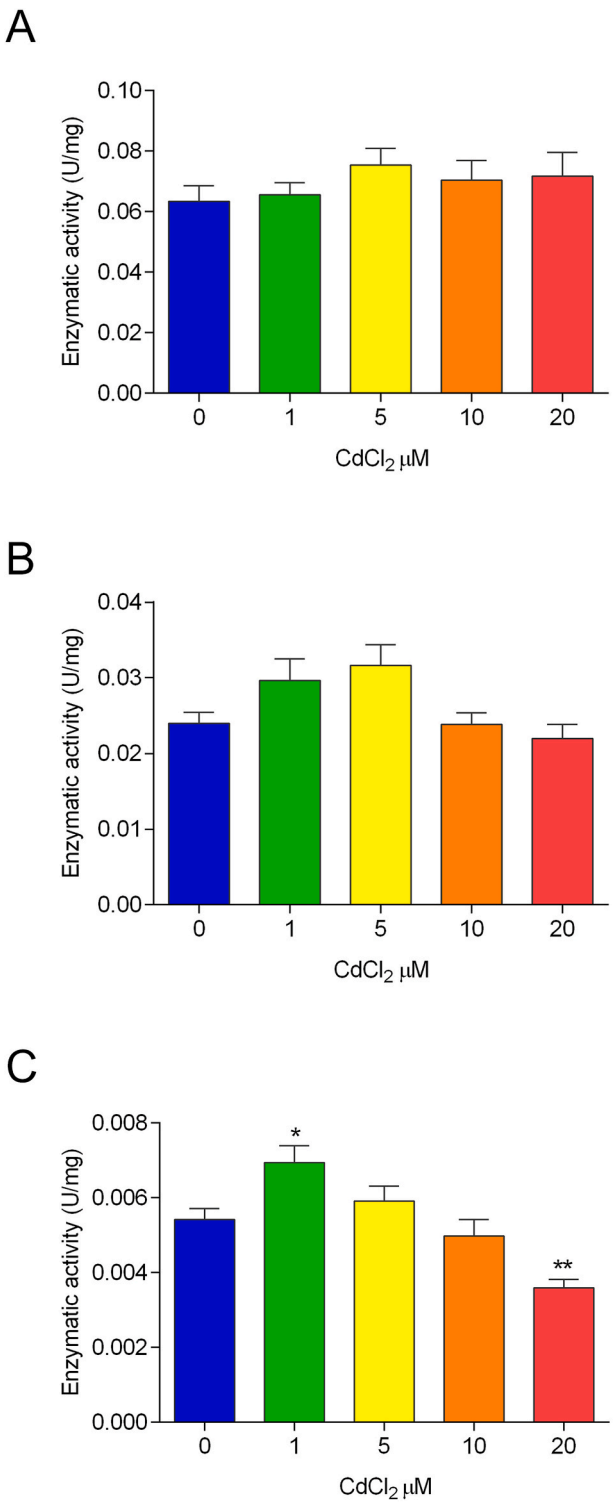

Fig. 7. Enzyme activities of glucose 6-phosphate dehydrogenase (A), isocitrate dehydrogenase (B) and malic enzyme (C) in BV2 control and cadmium treated cells. Bars indicate the mean ± SEM of three biological replicates. *$p < 0.05$, **$p < 0.01$ for all graphs.

mRNA level, while treatment with 10 μM $CdCl_2$ caused a significant increase in both IL-6 and IL-1β. On the other hand, the mRNA level of TNFα, IL-4 and IL-10 remained comparable to control cells (Fig. 8A). Moreover, Iba1 evaluation through Western blot analysis showed an increase in its expression only at 10 μM $CdCl_2$, remaining similar to control for all the other conditions tested (Fig. 8B).

4. Discussion

This work was prompted by the interest in the toxic effect of sublethal cadmium concentration on glial cells, a possible player in neurodegenerative disease pathogenesis. Cadmium is well known to be toxic at high concentrations, however its toxicity towards neuronal cells is often due to a chronic intoxication with sublethal amounts. Chronic exposure through different ways (e.g., ingestion of contaminated food and water, and inhalation) along with cadmium bioaccumulation and persistence (25–30 years) pose serious concerns, given that inside the cells cadmium can reach concentrations as high as 20 μM (Abu-Hayyeh et al., 2001; Forcella et al., 2020; Mezynska and Brzoska, 2018). In addition, recent advances (Hester et al., 2022; Saucier et al., 2023) show the possible correlation between environmental factors and neurodegenerative diseases, such as amyotrophic lateral sclerosis (ALS).

Heavy metals have been frequently associated with different neurodegenerative diseases pathogenesis; however, despite the many data available on cadmium toxicity, a detailed picture of cadmium toxicology on glial cells is still lacking, especially concerning cadmium effect on cell metabolism (Murumulla et al., 2023).

The first experiments reported in this paper show that low cadmium concentrations cause a progressive reduction in cell density, as well as morphological changes. Although no differences were observed between control cells and those treated with the lowest cadmium concentration, at the higher concentrations used a progressive reduction in cell density and an increase in the number of cells showing blebs formations with a more irregular morphology could be observed. The changes in cell morphology, as well as cellular heterogeneity, were also confirmed in confocal microscopy, through tubulin, nuclei and mitochondrial staining. Confocal microscopy also showed that cadmium induced mitochondria relocalization around the nucleus, as previously observed in C3H murine fibroblasts treated with sublethal cadmium concentrations (Oldani et al., 2020).

A linear increase in metallothioneins and HMOX1 upregulation was also observed in glial BV2 cells at increasing cadmium concentrations. However, in these cells oxidative stress is more efficiently kept under control by the upregulation of both glutathione S-transferase and glutathione reductase, increasing the rate of glutathione reduction. This is particularly important to efficiently scavenge cytosolic hydrogen peroxide which might react with iron, released by HMOX1, leading to Fenton reaction. Interestingly, neither the total amount of glutathione nor the expression of glucose 6 phosphate dehydrogenase vary upon cadmium administration, suggesting that no additional glutathione or NADPH is required to balance oxidative stress.

1 μM cadmium concentration already upregulates metallothioneins and is sufficient to induce an increase in mitochondrial electron transport and ATP production. Pyruvate kinase expression also starts to increase at this concentration, as well as the malic enzyme, which returns to normal values at higher cadmium concentrations; this could be indicative of an excess of citrate being carried into the cytosol for lipogenesis (Chausse et al., 2021).

5 μM cadmium leads to oxidative stress, with increased lipid peroxidation and reduced glutathione depletion. Pyruvate kinase, lactate dehydrogenase and malate dehydrogenase expression also increase following 5 μM cadmium administration; however, while lactate dehydrogenase and malate dehydrogenase return to initial values at higher cadmium concentrations, suggesting that no variations take place in lactic fermentation and Krebs cycle, pyruvate kinase activity continues to increase. This suggests a moderate glycolysis upregulation accompanied by an excess NADH which must be reoxidized, in order for the pathway to carry on.

At 10 μM cadmium concentration, lipid peroxidation has substantially decreased, thanks to the upregulation of both glutathione S-transferase and glutathione reductase activities, repleting reduced glutathione. Moreover, at this cadmium concentration, new rearrangements are observed: ATP level starts to decrease, together with

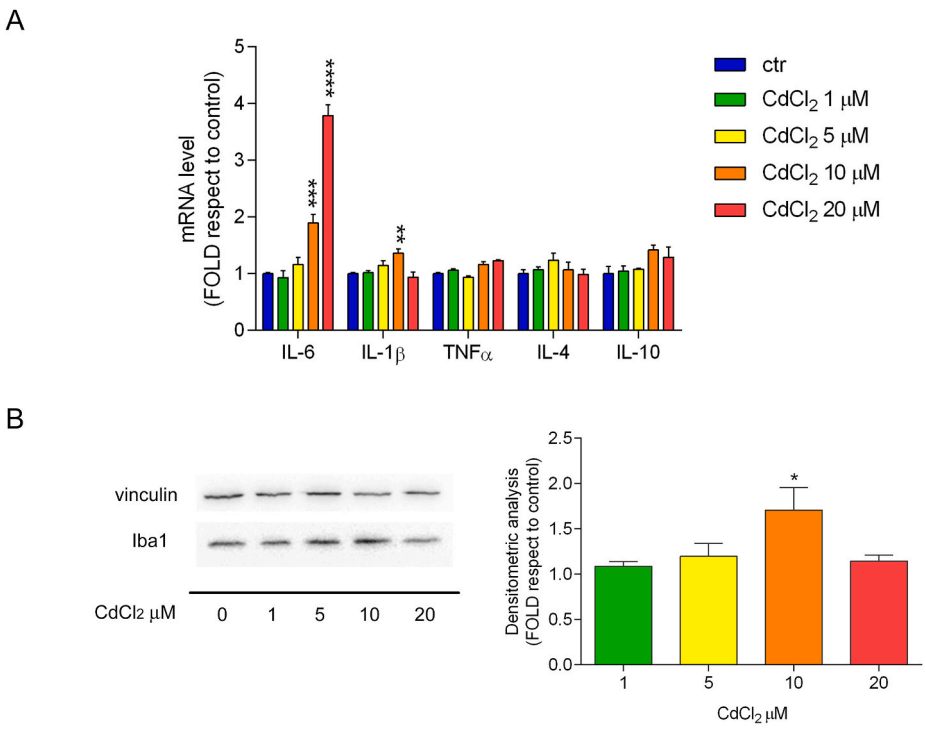

Fig. 8. (A) Pro-inflammatory, IL-6, IL-1β and TNFα, and anti-inflammatory, IL-4 and IL-10, cytokines mRNA level in cadmium treated cells. (B) Representative Western blot analysis of Iba1 and its expression level in metal treated cells expressed as fold compared to control. Bars indicate the mean ± SEM of three biological replicates. *p < 0.05, **p < 0.01, ***p < 0.001, ****p < 0.0001 for all graphs.

mitochondrial functionality. Also, proinflammatory signals, such as Il-6, Il-1β and Iba1, are released from BV2 cells, suggesting that cadmium can induce an inflammatory state.

Finally, at 20 μM cadmium, ATP production further decreases, mitochondria becoming dysfunctional, both glycolytic capacity and glycolytic reserve also decrease, while metallothioneins, HMOX1, glutathione S-transferase and glutathione reductase levels continue to increase. Conversely, lipid peroxidation reaches the lowest level, showing that these enzymes effectively contrast oxidative stress. A concentration of 20 μM can be considered toxic, however interestingly the surviving cells respond to cadmium toxicity by increasing metallothioneins expression, as well as their antioxidative responses. Mitochondrial dysfunction and impairment of oxidative phosphorylation likely lead cells to death.

As for oxidative metabolism, Seahorse experiments show that besides the upregulation of basal and maximal respirations and oxidative phosphorylation which are observed at 1 μM cadmium, these parameters tend to decrease, although not significantly (except for the values at 20 μM cadmium). This suggests possible mitochondrial damage, which is not compensated by glycolysis, since ATP produced in this pathway starts to significantly decrease at 10 μM cadmium. Neither glycolysis nor oxidative phosphorylation are significantly affected by cadmium up to 10 μM.

During chronic exposure to cadmium, its concentration can increase substantially during the years; thus, the metabolic alterations we have observed in BV2 cultured cells are likely to be found also in vivo. In fact, cadmium is a very common pollutant which, apart from occupational exposure, is easily uptaken through ingestion of contaminated food and water, inhalation of polluted air, and cigarette smoke, with concentrations up to 20 μM being reported in smokers (Abu-Hayyeh et al., 2001).

In a previous paper (Bovio et al., 2021), we reported the effect of sublethal cadmium concentrations on human SH-SY5Y neuronal cells metabolism, showing that cadmium exacerbates the Warburg effect, decreasing mitochondria functionality and increasing glutamine uptake for lipid biosynthesis. We also showed that glutathione is an essential defense against the oxidative stress caused by cadmium administration; the cause-effect relationship between cadmium and oxidative stress is further confirmed by the fact that, when two antioxidants, GSH and cysteine, were separately administered to BV2 cultured cells, pretreatment with either GSH or Cysteine allowed the cells to maintain a 100% viability, at $CdCl_2$ concentrations up to 20 μM (data not shown). This strongly suggests that each antioxidant fully protects BV2 cells from oxidative stress induced by $CdCl_2$ at concentrations up to 20 μM. At 50 μM $CdCl_2$ pretreatment with each antioxidant still leads to a 50% increase in cell viability compared to control untreated cells.

Although in our previous experiments, SH-SY5Y cells increased glutathione synthesis when treated with cadmium, at both 10 μM and 20 μM $CdCl_2$ GSH was not sufficient to counterbalance the increase in oxidative stress induced by this metal. Respect to neuronal SH-SY5Y cells, BV2 cells appear to be more resistant to oxidative stress and to already have adequate amounts of both NADPH and GSH, which are not increased upon cadmium administration. The increase in oxidative stress induced by cadmium is managed by an increase in the activity of both GST and GR. BV2 cells may therefore play a key role in neuroprotection against cadmium toxicity, also considering that glutathione is normally released by glia and uptaken by neurons. However, while in astrocytes GSH synthesis plays a role in supporting neurons, in microglial cells GSH is exclusively used to eliminate ROS generated under pathological conditions, so that GSH level and GR activity are higher in cultured microglia compared to astrocytes (Hirrlinger et al., 2000).

Our data do not suggest that cadmium can markedly induce a shift of BV2 cells towards the M1 phenotype. Some events characterizing the shift do take place, such as inflammatory cytokines release and increased glycolysis; however, in our experiments the increase in glycolytic capacity and glycolytic reserve at 1 μM cadmium was not found statistically significant, so that a Warburg effect was not observed. This is also confirmed by the fact that neither PKM2 nor PFKFB3 expression are increased, as they normally are in the Warburg effect. The release of proinflammatory signals by BV2 cells exposed to cadmium, suggest a possible role in the biochemistry of neuroinflammation

processes and a contribution of these cells to neuronal damage. Future experiments will shed more light on this interaction and on the dynamics of the neuroinflammatory process.

This work, along with our previous published papers, is a first step to characterize mitochondria involvement in the processes of neurotoxicity and its possible role in neurodegeneration during exposure to environmental factors, such as metals. The second step, namely co-cultures of microglial and neuronal cell lines, will provide important cues to the understanding of cadmium, and environmental factors in general, as key players in neurodegeneration and to the understanding of mechanistic aspects.

Credit author statement

Conceptualization: F.B., M.F., P.F.; Investigation: F.B., P.M., E.P.; Visualization: F.B., D.F., M.F.; Data curation: F.B.; Funding acquisition: P.F., C.U.; Project administration: M.F., P.F., C.U.; Resources: P.F., C.U., D.F.; Supervision: M.F.; Writing – original draft: F.B., M.F., P.F., C.U.; Writing – review & editing: F.B., M.F., E.P., D.F., P.F., C.U.All authors read and approved the final manuscript.

Funding

This work was supported by the University of Milano-Bicocca (2020-ATE-0270 to PF and 2020-ATE-043 to CU).

Declaration of competing interest

The authors declare that they have no known competing financial interests or personal relationships that could have appeared to influence the work reported in this paper.

Data availability

Data will be made available on request.

Acknowledgments

We thank Professor Maria D'Erme from University of Rome "La Sapienza" and Dr. Maddalena Grieco from Italian National Research Council (CNR), Rome for kindly donating the BV2 murine microglia cell line.

References

Abu-Hayyeh, S., Sian, M., Jones, K.G., Manuel, A., Powell, J.T., 2001. Cadmium accumulation in aortas of smokers. Arterioscler. Thromb. Vasc. Biol. 21, 863–867. https://doi.org/10.1161/01.ATV.21.5.863.

ATSDR, 2022. Support document to the 2022 substance priority list (candidates for toxicological profiles) agency for toxic substances and disease registry division of toxicology and human health sciences. December, 2022 1–12.

Bergmeyer, H.U., Gaweh, K., G, M., 1974. Enzymes as biochemical reagents. In: HU, B. (Ed.), Methods of Enzymatic Analysis. Academic Press, New York, pp. 427–522.

Borst, K., Schwabenland, M., Prinz, M., 2019. Microglia metabolism in health and disease. Neurochem. Int. 130, 104331 https://doi.org/10.1016/j.neuint.2018.11.006.

Bovio, F., Melchioretto, P., Forcella, M., Fusi, P., Urani, C., 2021. Cadmium promotes glycolysis upregulation and glutamine dependency in human neuronal cells. Neurochem. Int. 149, 105144 https://doi.org/10.1016/j.neuint.2021.105144.

Bradford, M.M., 1976. A rapid and sensitive method for the quantitation of microgram quantities of protein utilizing the principle of protein-dye binding. Anal. Biochem. 72, 248–254.

Branca, J.J.V., Fiorillo, C., Carrino, D., Paternostro, F., Taddei, N., Gulisano, M., Pacini, A., Becatti, M., 2020. Cadmium-induced oxidative stress: focus on the central nervous system. Antioxidants 9, 1–21. https://doi.org/10.3390/antiox9060492.

Brand, M.D., 2016. Mitochondrial generation of superoxide and hydrogen peroxide as the source of mitochondrial redox signaling. Free Radic. Biol. Med. 100, 14–31. https://doi.org/10.1016/j.freeradbiomed.2016.04.001.

Buege, J.A., Aust, S.D., 1978. Microsomal lipid peroxidation. Methods Enzymol. 52, 302–310. https://doi.org/10.1016/s0076-6879(78)52032-6.

Chausse, B., Kakimoto, P.A., Kann, O., 2021. Microglia and lipids: how metabolism controls brain innate immunity. Semin. Cell Dev. Biol. 112, 137–144. https://doi.org/10.1016/j.semcdb.2020.08.001.

Deng, P., Zhang, H., Wang, L., Jie, S., Zhao, Q., Chen, F., Yue, Y., Wang, H., Tian, L., Xie, J., Chen, M., Luo, Y., Yu, Z., Pi, H., Zhou, Z., 2023. Long-term cadmium exposure impairs cognitive function by activating lnc-Gm10532/m6A/FIS1 axis-mediated mitochondrial fission and dysfunction. Sci. Total Environ. 858, 159950 https://doi.org/10.1016/j.scitotenv.2022.159950.

Forcella, M., Lau, P., Fabbri, M., Fusi, P., Oldani, M., Melchioretto, P., Gribaldo, L., Urani, C., 2022. Is cadmium toxicity tissue-specific? Toxicogenomics studies reveal common and specific pathways in pulmonary, hepatic, and neuronal cell models. Int. J. Mol. Sci. 23 https://doi.org/10.3390/ijms23031768.

Forcella, M., Lau, P., Oldani, M., Melchioretto, P., Bogni, A., Gribaldo, L., Fusi, P., Urani, C., 2020. Neuronal specific and non-specific responses to cadmium possibly involved in neurodegeneration: a toxicogenomics study in a human neuronal cell model. Neurotoxicology 76, 162–173. https://doi.org/10.1016/j.neuro.2019.11.002.

Garner, R., Levallois, P., 2016. Cadmium levels and sources of exposure among Canadian adults. Heal. reports 27, 10–18.

Genchi, G., Sinicropi, M.S., Lauria, G., Carocci, A., Catalano, A., 2020. The effects of cadmium toxicity. Int. J. Environ. Res. Publ. Health 17. https://doi.org/10.3390/ijerph17113782.

Habig, W.H., Pabst, M.J., Jakoby, W.B., 1974. Glutathione S-transferases. The first enzymatic step in mercapturic acid formation. J. Biol. Chem. 249, 7130–7139.

Hartwig, A., Jahnke, G., 2017. [Metals and their compounds as contaminants in food : arsenic, cadmium, lead and aluminum]. Bundesgesundheitsblatt - Gesundheitsforsch. - Gesundheitsschutz 60, 715–721. https://doi.org/10.1007/s00103-017-2567-0.

Henn, A., Lund, S., Hedtjärn, M., Schrattenholz, A., Pörzgen, P., Leist, M., 2009. The suitability of BV2 cells as alternative model system for primary microglia cultures or for animal experiments examining brain inflammation. ALTEX 26, 83–94. https://doi.org/10.14573/altex.2009.2.83.

Hester, K., Kirrane, E., Anderson, T., Kulikowski, N., Simmons, J.E., Lehmann, D.M., 2022. Environmental exposure to metals and the development of tauopathies, synucleinopathies, and TDP-43 proteinopathies: a systematic evidence map protocol. Environ. Int. 169, 107528 https://doi.org/10.1016/j.envint.2022.107528.

Hirrlinger, J., Gutterer, J.M., Kussmaul, L., Hamprecht, B., Dringen, R., 2000. Microglial cells in culture express a prominent glutathione system for the defense against reactive oxygen species. Dev. Neurosci. 22, 384–392. https://doi.org/10.1159/000017464.

Khan, A., Ikram, M., Muhammad, T., Park, J., Kim, M.O., 2019. Caffeine modulates cadmium-induced oxidative stress, neuroinflammation, and cognitive impairments by regulating nrf-2/HO-1 in vivo and in vitro. J. Clin. Med. 8 https://doi.org/10.3390/jcm8050680.

Kim-Lee, M.H., Stokes, B.T., Yates, A.J., 1992. Reperfusion paradox: a novel mode of glial cell injury. Glia 5, 56–64. https://doi.org/10.1002/glia.440050109.

Laemmli, 1970. Cleavage of structural proteins during the assembly of the head of bacteriophage T4. Nature 227, 680–685.

Lillehoj, E.P., Guang, W., Hyun, S.W., Liu, A., Hegerle, N., Simon, R., Cross, A.S., Ishida, H., Luzina, I.G., Atamas, S.P., Goldblum, S.E., 2019. Neuraminidase 1-mediated desialylation of the mucin 1 ectodomain releases a decoy receptor that protects against Pseudomonas aeruginosa lung infection. J. Biol. Chem. 294, 662–678. https://doi.org/10.1074/jbc.RA118.006022.

Liu, S., Yu, D., Wei, P., Cai, J., Xu, M., He, H., Tang, X., Nong, C., Wei, Y., Xu, X., Mo, X., Zhang, Z., Qin, J., 2023. JAK2/STAT3 signaling pathway and klotho gene in cadmium-induced neurotoxicity in vitro and in vivo. Biol. Trace Elem. Res. 201, 2854–2863. https://doi.org/10.1007/s12011-022-03370-9.

Livak, K.J., Schmittgen, T.D., 2001. Analysis of relative gene expression data using real-time quantitative PCR and the 2(-Delta Delta C(T)) Method. Methods 25, 402–408 [pii].

Ma, Y., Su, Q., Yue, C., Zou, H., Zhu, J., Zhao, H., Song, R., Liu, Z., 2022. The effect of oxidative stress-induced autophagy by cadmium exposure in kidney, liver, and bone damage, and neurotoxicity. Int. J. Mol. Sci. 23 https://doi.org/10.3390/ijms232113491.

Martelli, A., Rousselet, E., Dycke, C., Bouron, A., Moulis, J.M., 2006. Cadmium toxicity in animal cells by interference with essential metals. Biochimie 88, 1807–1814. https://doi.org/10.1016/j.biochi.2006.05.013.

Martínez-Hernández, M.I., Acosta-Saavedra, L.C., Hernández-Kelly, L.C., Loaeza-Loaeza, J., Ortega, A., 2023. Microglial activation in metal neurotoxicity: impact in neurodegenerative diseases. BioMed Res. Int. 2023, 7389508 https://doi.org/10.1155/2023/7389508.

Mezynska, M., Brzoska, M.M., 2018. Environmental exposure to cadmium-a risk for health of the general population in industrialized countries and preventive strategies. Environ. Sci. Pollut. Res. Int. 25, 3211–3232. https://doi.org/10.1007/s11356-017-0827-z.

Murumulla, L., Bandaru, L.J.M., Challa, S., 2023. Heavy metal mediated progressive degeneration and its noxious effects on brain microenvironment. Biol. Trace Elem. Res. https://doi.org/10.1007/s12011-023-03778-x.

Oggiano, R., Pisano, A., Sabalic, A., Farace, C., Fenu, G., Lintas, S., Forte, G., Bocca, B., Madeddu, R., 2021. An overview on amyotrophic lateral sclerosis and cadmium. Neurol. Sci. Off. J. Ital. Neurol. Soc. Ital. Soc. Clin. Neurophysiol. 42, 531–537. https://doi.org/10.1007/s10072-020-04957-7.

Oldani, M., Manzoni, M., Villa, A.M., Stefanini, F.M., Melchioretto, P., Monti, E., Forcella, M., Urani, C., Fusi, P., 2020. Cadmium elicits alterations in mitochondrial morphology and functionality in C3H10T1/2Cl8 mouse embryonic fibroblasts.

Biochim. Biophys. Acta - Gen. Subj. 1864, 129568 https://doi.org/10.1016/j.bbagen.2020.129568.
Pamphlett, R., Bishop, D.P., Kum Jew, S., Doble, P.A., 2018. Age-related accumulation of toxic metals in the human locus ceruleus. PLoS One 13, e0203627. https://doi.org/10.1371/journal.pone.0203627.
Rangaraju, S., Dammer, E.B., Raza, S.A., Gao, T., Xiao, H., Betarbet, R., Duong, D.M., Webster, J.A., Hales, C.M., Lah, J.J., Levey, A.I., Seyfried, N.T., 2018. Quantitative proteomics of acutely-isolated mouse microglia identifies novel immune Alzheimer's disease-related proteins. Mol. Neurodegener. 13, 34. https://doi.org/10.1186/s13024-018-0266-4.
Ruczaj, A., Brzóska, M.M., 2023. Environmental exposure of the general population to cadmium as a risk factor of the damage to the nervous system: a critical review of current data. J. Appl. Toxicol. 43, 66–88. https://doi.org/10.1002/jat.4322.
Sarchielli, E., Pacini, S., Morucci, G., Punzi, T., Marini, M., Vannelli, G.B., Gulisano, M., 2012. Cadmium induces alterations in the human spinal cord morphogenesis. Biometals an Int. J. role Met. ions Biol. Biochem. Med. 25, 63–74. https://doi.org/10.1007/s10534-011-9483-9.
Sarkar, A., Ravindran, G., Krishnamurthy, V., 2013. A brief review on the effect of cadmium toxicity: from cellular to organ level. Int. J. Bio Technol. Res. 3, 2249–6858.
Sarwar, N., Malhi, S.S., Zia, M.H., Naeem, A., Bibi, S., Farid, G., 2010. Role of mineral nutrition in minimizing cadmium accumulation by plants. J. Sci. Food Agric. 90, 925–937. https://doi.org/10.1002/jsfa.3916.
Sasaki, N., Carpenter, D.O., 2022. Associations between metal exposures and cognitive function in American older adults. Int. J. Environ. Res. Publ. Health 19. https://doi.org/10.3390/ijerph19042327.
Saucier, D., Registe, P.P.W., Bélanger, M., O'Connell, C., 2023. Urbanization, air pollution, and water pollution: identification of potential environmental risk factors associated with amyotrophic lateral sclerosis using systematic reviews. Front. Neurol. https://doi.org/10.3389/fneur.2023.1108383.
Smith, P.K., Krohn, R.I., Hermanson, G.T., Mallia, A.K., Gartner, F.H., Provenzano, M.D., Fujimoto, E.K., Goeke, N.M., Olson, B.J., Klenk, D.C., 1985. Measurement of protein using bicinchoninic acid. Anal. Biochem. 150, 76–85. https://doi.org/10.1016/0003-2697(85)90442-7.
Sunderman, F.W.J., 2001. Nasal toxicity, carcinogenicity, and olfactory uptake of metals. Ann. Clin. Lab. Sci. 31, 3–24.
Tang, J., Duan, W., Deng, P., Li, H., Liu, C., Duan, Y., Feng, M., Xu, S., 2021. Cadmium disrupts mitochondrial distribution and activates excessive mitochondrial fission by elevating cytosolic calcium independent of MCU-mediated mitochondrial calcium uptake in its neurotoxicity. Toxicology 453, 152726. https://doi.org/10.1016/j.tox.2021.152726.
Thévenod, F., Fels, J., Lee, W.K., Zarbock, R., 2019. Channels, transporters and receptors for cadmium and cadmium complexes in eukaryotic cells: myths and facts. Biometals 32, 469–489. https://doi.org/10.1007/s10534-019-00176-6.
Urani, C., Melchioretto, P., Gribaldo, L., 2010. Regulation of metallothioneins and ZnT-1 transporter expression in human hepatoma cells HepG2 exposed to zinc and cadmium. Toxicol. Vitro 24, 370–374. https://doi.org/10.1016/j.tiv.2009.11.003.
Wang, B., Du, Y., 2013. Cadmium and its neurotoxic effects. Oxid. Med. Cell. Longev. 2013, 898034 https://doi.org/10.1155/2013/898034.
Wang, H., Matsushita, M.T., 2021. Heavy metals and adult neurogenesis. Curr. Opin. Toxicol. 26, 14–21. https://doi.org/10.1016/j.cotox.2021.03.006.
Wang, Y., Oberley, L.W., Murhammer, D.W., 2001. Antioxidant defense systems of two lipidopteran insect cell lines. Free Radic. Biol. Med. 30, 1254–1262. https://doi.org/10.1016/s0891-5849(01)00520-2.
Wen, S., Xu, M., Zhang, W., Song, R., Zou, H., Gu, J., Liu, X., Bian, J., Liu, Z., Yuan, Y., 2023. Cadmium induces mitochondrial dysfunction via SIRT1 suppression-mediated oxidative stress in neuronal cells. Environ. Toxicol. 38, 743–753. https://doi.org/10.1002/tox.23724.
Wright-Jin, E.C., Gutmann, D.H., 2019. Microglia as dynamic cellular mediators of brain function. Trends Mol. Med. 25, 967–979. https://doi.org/10.1016/j.molmed.2019.08.013.
Xu, Y., Liu, J., Tian, Y., Wang, Z., Song, Z., Li, K., Zhang, S., Zhao, H., 2022. Wnt/β-Catenin signaling pathway is strongly implicated in cadmium-induced developmental neurotoxicity and neuroinflammation: clues from zebrafish neurobehavior and in vivo neuroimaging. Int. J. Mol. Sci. 23 https://doi.org/10.3390/ijms231911434.
Yang, Z., Yang, S., Qian, S.Y., Hong, J.-S., Kadiiska, M.B., Tennant, R.W., Waalkes, M.P., Liu, J., 2007. Cadmium-induced toxicity in rat primary mid-brain neuroglia cultures: role of oxidative stress from microglia. Toxicol. Sci. 98, 488–494. https://doi.org/10.1093/toxsci/kfm106.